MATERIALS CHEMISTRY FRONTIERS

CHINESE CHEMICAL SOCIETY

ROYAL SOCIETY OF CHEMISTRY

RESEARCH ARTICLE

View Article Online
View Journal | View Issue

Open Access Article. Published on 06 September 2024. Downloaded on 1/22/2026 4:13:36 PM.
This article is licensed under a Creative Commons Attribution-NonCommercial 3.0 Unported Licence.

Check for updates

Cite this: *Mater. Chem. Front.*, 2024, **8**, 3799

Dual luminescence and infrared circularly polarized luminescence up to 900 nm with platinum complexes bearing a helical donor–acceptor ligand†

Pablo Vázquez-Domínguez, ‡[ab] Maher Horojat,‡[c] Eva Suits,[a] Francisco José Fernández de Córdova,[a] Nicolas Vanthuyne,[d] Denis Jacquemin,*[ef] Abel Ros*[a] and Ludovic Favereau*[c]

Received 25th July 2024,
Accepted 29th August 2024

DOI: 10.1039/d4qm00632a

rsc.li/frontiers-materials

Chiral molecular materials able to emit circularly polarized luminescence (CPL) have attracted considerable interest in the last few decades, due to the potential of CP-light in a wide range of applications. While CP luminescent molecules with blue, green, and yellow emissions are now well-reported, NIR CPL from organic and organometallic compounds lags behind due to the dual challenge of promoting radiative deexcitation of the excited state in this low energy region while assuring a significant magnetic dipole transition moment, a prerequisite for generating CPL. Based on a versatile axially chiral arylisoquinoline ligand, we report the synthesis and chiroptical properties of chiral donor–acceptor platinum(II) complexes displaying CPL that extends up to almost 900 nm. Interestingly, these emitters show both fluorescence and phosphorescence emissions in solution, with intensities depending on the charge-transfer character of the organic ligand. Experimental and theoretical investigations show that this feature strongly impacts the intersystem crossing event between the singlet and triplet excited states of these complexes and the related phosphorescence lifetime. The effect is less important regarding the CPL, and most complexes show luminescence dissymmetry factors with values up to *ca.* 2×10^{-3} around 800 nm.

Introduction

Molecular compounds able to emit in the near infrared region (NIR) of the electromagnetic spectrum attract intense interest due to their potential applications, ranging from optoelectronics to bioimagery. During the last decade, the development of chiral emitters able to display circularly polarized luminescence (CPL) has motivated chemists working in this area to develop NIR CPL compounds. Indeed, CP-light displays potential advantages over its non-polarized counterpart in the aforementioned applications, such as in organic light-emitting diodes (OLEDs), CP light detectors, as well as in chiral sensing and bioimaging.[1–7]

Accordingly, the design of NIR CPL emitters has emerged with lanthanides and chromium complexes constituting the first compounds reaching high intensity of CPL thanks to their magnetically allowed and electrically forbidden transitions.[1,8–12] In a complementary strategy, chiral molecular organic and organometallic complexes have also been investigated due to their readily tuneable optoelectronic properties, simple processability, and often higher photoluminescence quantum yields (PLQYs). The latter aspect, associated with the high molar extinction coefficient of the related electric dipole-allowed transitions, provide this class of chiral complexes with potentially high CPL brightness.[13,14] These features make these dyes valuable candidates for CPL applications,[15–22] with promising examples of blue, green, and yellow CPL emitters.[23] However, reaching the far red, and even the NIR remains a considerable challenge for both organic and organometallic derivatives,[24] since the competition with nonradiative deactivation pathways of the excited state is the first aspect to overcome, commonly underlined by the so-called 'energy gap law'. In addition, the needed electronic and structural factors for reaching this low-energy emission, *i.e.*, a delocalized

[a] *Institute for Chemical Research (CSIC-US) C/Américo Vespucio 49, E-41092 Seville, Spain. E-mail: abel.ros@iiq.csic.es*
[b] *Department of Organic Chemistry, Innovation Centre in Advanced Chemistry, ORFEO-CINQA, University of Seville, C/Prof. García González 1, 41012 Seville, Spain*
[c] *Univ Rennes, CNRS, ISCR-UMR 6226, F-35000 Rennes, France. E-mail: ludovic.favereau@univ-rennes.fr*
[d] *Aix Marseille University, CNRS, Centrale Marseille, iSm2, Marseille, France*
[e] *Nantes Université, CNRS, CEISAM UMR 6230, F-44000 Nantes, France. E-mail: Denis.Jacquemin@univ-nantes.fr*
[f] *Institut Universitaire de France (IUF), F-75005, Paris, France*

† Electronic supplementary information (ESI) available. CCDC 2373489 and 2373501. For ESI and crystallographic data in CIF or other electronic format see DOI: https://doi.org/10.1039/d4qm00632a

‡ These authors contributed equally

Open Access Article. Published on 06 September 2024. Downloaded on 1/22/2026 4:13:36 PM.
This article is licensed under a Creative Commons Attribution-NonCommercial 3.0 Unported Licence.

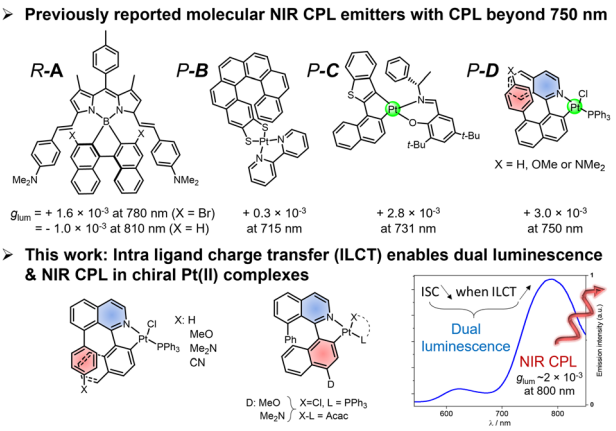

Fig. 1 Top: Chemical structures of the molecular CPL emitters displaying CPL maxima beyond 750 nm in solution. Bottom: Chemical structures of the investigated helical donor–acceptor platinum(II) complexes in this report.

π-conjugated system with often a rigid and planar molecular backbone, are usually hardly compatible with a significant magnetic (m) dipole transition moment, a prerequisite for chiroptical properties such as CPL.

While elegant designs of helical organic and organometallic systems have shown CPL in the red and far-red region,[25–34] only a few examples have currently achieved a CPL over 750 nm (Fig. 1).[35,36] For these, the obtained luminescence dissymmetry factor, g_{lum}, remains rather modest with values rarely larger than 3×10^{-3}. The investigated molecular designs are either based on an extended π-conjugated chromophoric unit based on BODIPY (A, Fig. 1) or rely on platinum complexes incorporating chiral ligands such as carbohelicene.[36–43] Indeed, Pt complexes have been found to be promising to generate NIR phosphorescence, with cyclometalated phosphorescent d^8 metal complexes extensively studied for the development of high-performance far red and NIR-OLEDs.[36,42,44]

Following this line of research, we recently reported a new family of chiral donor–acceptor platinum(II) complexes involving an organic helical ligand possessing a significant intramolecular charge-transfer (ICT) character.[45] This feature affords a dual luminescence behaviour with a fluorescence emission arising from the ligand and a NIR phosphorescence that can be modulated by the ICT character of the helical ligand. Interestingly, these complexes exhibit NIR CP phosphorescence with a g_{lum} of 3×10^{-3}, a significant value in this low energy region. While these results highlight interesting aspects regarding the design of NIR CPL emitters, such "helical donor–acceptor platinum complex design" remains limited to a few examples only, hampering a clear rationalization of the dual luminescence process and its implication on the possibility to reach NIR CPL. Accordingly, we decided to synthesize a complete family of chiral platinum complexes to explore the structural and electronic impact of the electron donating groups on the dual fluorescence/phosphorescence emissions as well as on the associated CPL signals.

We report here on the synthesis, photophysical, and chiroptical properties of a new family of NIR CPL helical donor–acceptor platinum complexes based on axially chiral arylisoquinoline ligands. Playing with the functionalization of either the isoquinoline or the naphthyl unit of these molecular systems strongly impacts both the photophysical and chiroptical properties, by notably promoting dual luminescence emission and NIR CPL extending up to 900 nm. Experimental and theoretical investigations revealed that this effect is related to a subtle interplay between the ILCT transition localized on the ligand and the MLCT one involving the metallic centre, with a dual emission process becoming more favoured when electron donor substituents are attached to the naphthyl core. Such an impact is however less pronounced on the chiroptical properties and NIR CPL can be detected for most of the complexes with a promising g_{lum} of up to *ca.* 2×10^{-3} around 800 nm.

Results and discussion

Synthesis and characterization

Based on our previous results[45] and with the idea of developing a new family of CPL active Pt-based complexes with NIR-luminescence, we decided to modify the structure of the N,C-ligands by introducing aryl moieties with different electron richness to control the balance between the ILCT and MLCT transitions and tune the resulting emission process. Initially, the synthesis of the [Pt(N,C)(PPh_3)Cl] complexes **1–4** containing an aryl substituent at the 8-position of isoquinoline was carried out (Scheme 1a). Starting from the free ligands **L1–L2** (see the ESI†), a cyclometallation step followed by a ligand replacement (DMSO → PPh_3), affords the desired complexes **1–4** in excellent yields.[40,46–48] These complexes were completely characterized by NMR and HRMS (see the ESI†) and were found to be stable to oxygen and moisture, being purified by flash chromatography on silica gel. The X-ray structure for (±)-**2** (Scheme 1b) clearly shows the expected helicoidal disposition of the ligand (aryl···aryl distance of 3.016 Å) and the *trans* configuration between the phosphine moiety and the nitrogen atom (Pt–P distance of 2.234 Å) which fits with the solution-phase observation ($^1J_{Pt,P}$ = 4454 Hz).

Along the same lines, we decided to analyse the effect of changing the naphthalene ring on complex **1** by more electron rich substituents by introducing an electron donating groups like –OMe and –NMe_2 at the 4-position of the naphthalene

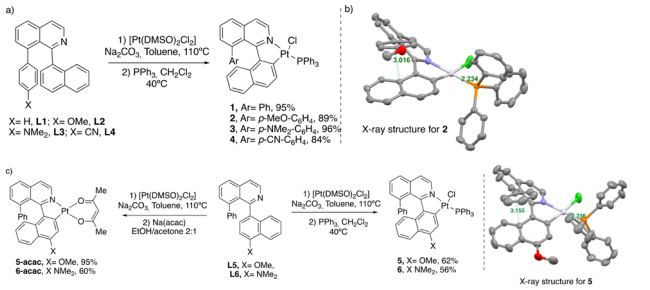

Scheme 1 (a) Synthesis of the Pt-complexes **1–4**. (b) X-ray structure of **2**; (c) synthesis of the Pt-complexes **5–6** and their corresponding acetylacetone (acac), with the corresponding X-ray structure of (±)-**5**.

Open Access Article. Published on 06 September 2024. Downloaded on 1/22/2026 4:13:36 PM.
This article is licensed under a Creative Commons Attribution-NonCommercial 3.0 Unported Licence.

fragment (Scheme 1c). Following the same synthetic strategy, the corresponding complexes **5–6** were obtained in modest 56–62% yields as orange to purple solids. Finally, we decided to study the effect of replacing the 3D dimensional bulky triphenylphosphine ligand with a bidentate anionic ligand such as acac, *i.e.*, acetylacetonate, with the aim of increasing the planarity of the complexes, and therefore, to increase π···π and Pt···Pt intermolecular interactions. Following a similar strategy, ligands **L5–L6** were used in the cyclometalation step to give the corresponding [Pt(N,C)(DMSO)Cl] intermediates which, after reaction with Na(acac), afforded the final **5-acac–6-acac** complexes in 60–95% yields as pink to red solids.

The racemic complexes were resolved using semi-preparative chiral HPLC separation to give the enantiopure compounds with ee values up to 99% (see the ESI† for details). Their absolute configuration was assigned by comparison of their ECD responses with those of previously reported complexes[47] and further confirmed by theoretical calculations (see later). All products were characterized by ^{1}H and ^{13}C NMR spectroscopy and HRMS (see the ESI†).

Ground- and excited-state photophysical properties

In line with our recent study on Pt-based complexes with NIR-CPL,[45] we investigate here the structural and electronic parameters influencing the photophysical and chiroptical properties of these new chiral compounds, namely: (1) the impact of the donor position on the π-helical ligand and the resulting chiroptical properties for both the ground and excited states and (2) the magnitude of the intra ligand charge transfer and its interaction with the metal to ligand one, influencing the dual emission process and the efficiency of the NIR phosphorescence emission (*vide infra*). As depicted in Fig. 2, the absorption spectra of complexes **1–4** display similar profiles with two intense bands around 350 and 390 nm ($\varepsilon \sim 10 \times 10^3$ M^{-1} cm^{-1}) that are assigned to ligand π → π* transitions and a lowest energy broad signal between 420 and 530 nm ($\varepsilon \sim 4$–7×10^3 M^{-1} cm^{-1}) that involves both the metal and the ligand, *i.e.*, that can be characterized as a mixture of metal-to-ligand (ML) and intra-ligand (IL) charge-transfer excitations (for comparison, the UV-vis spectra of the corresponding organic ligands are depicted in Fig. S1 (ESI†). This assignment is supported by theoretical calculations, see the electron density difference (EDD) plots in Fig. 2 and Table S1 (ESI†).

Despite the difference in the donating/accepting electron ability of the functional groups at the 8-position of the isoquinoline fragment in these systems, the lowest absorption band shows only a minor shift, indicating a small effect of the substitution on the excited-state energies. This is easily

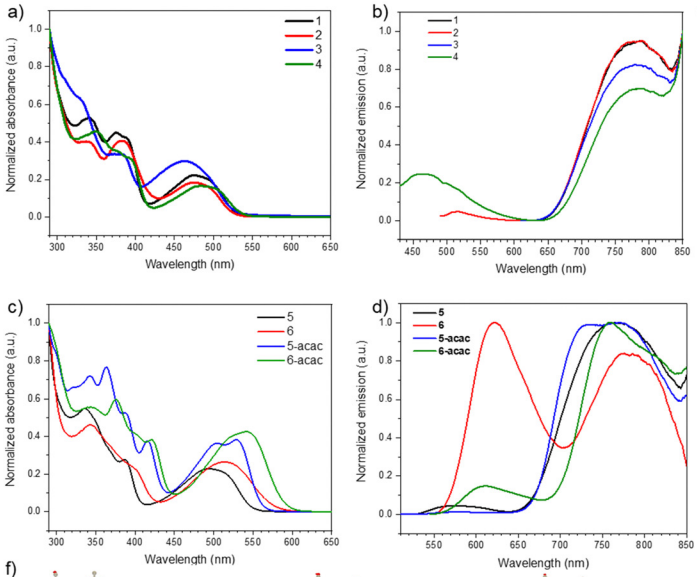

e)

	Absorption	Emission		Lifetime (ns)				SOC (in cm^{-1}) Gap in eV	
	λ_{max} (nm) / ε	λ_{em}^{fluo} (nm)	λ_{em}^{phos} (nm)	Aerated		degassed		S_1-T_1	S_1-T_2
1	475 / 4300	n.d.	788	n.d.	181.8	n.d.	453.1	14.1 -0.77	97.1 +0.22
2	493 / 4600	513	790	n.d.	177.2	n.d.	443.0	15.7 -0.77	94.0 +0.12
3	463 / 7200	n.d.	779	n.d.	178.9	n.d.	453.8	16.2 -0.77	74.3 -0.02
4	483 / 4000	464	787	2.40	196.2	2.03	491.7	16.5 -0.74	98.1 +0.22
5	475 / 4100	575	764	n.d.	285.5	n.d.	1992.4	10.7 -0.73	66.1 +0.31
6	515 / 5300	621	776	n.d.	245.8	n.d.	2398.8	7.8 -0.70	53.0 +0.34
5-acac	529 / 7500	579	730/769	n.d.	225.9	n.d.	1552.9	22.5 -0.71	144.1 +0.36
6-acac	542 / 10400	610	757	2.42	213.1	2.71	2106.7	16.6 -0.72	59.3 +0.40

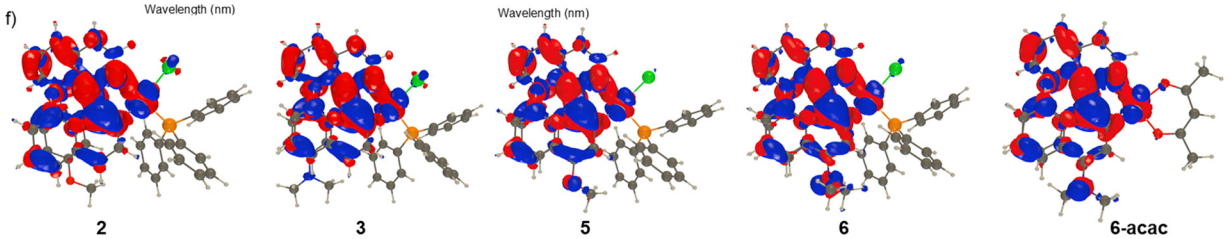

Fig. 2 (a) Normalized absorption and (b) emission spectra of complexes **1**, **2**, **3**, and **4** in toluene at 298 K; (c) normalized absorption and (d) emission spectra of complexes of complexes **5**, **5-acac**, **6**, and **6-acac** in toluene at 298 K; (e) photophysical data of the platinum complexes recorded in toluene at 298 K, under aerated and degassed conditions, with the corresponding lifetimes for the fluorescence and phosphorescence emissions (n.d.: not detected); S_1–T_1 and S_1–T_2 gaps (in eV) computed on the optimal S_1 geometries together with the associated SOCs (in cm^{-1}); (f) electron density difference plots for the lowest absorption of complexes **2**, **3**, **5**, **6** and **6-acac**. The blue (red) lobes correspond to region of decrease (increase) of density upon excitation. Contour threshold: 0.001 au (see the ESI† for details).

Open Access Article. Published on 06 September 2024. Downloaded on 1/22/2026 4:13:36 PM.
This article is licensed under a Creative Commons Attribution-NonCommercial 3.0 Unported Licence.

understandable by the EDD plots that all show almost no involvement of the substituent at 8-position in the lowest excited state. This can look surprising, especially for **3** that bears a potent NMe_2 group. However, the expected IL-CT in which this group acts as a strong donor is actually the second state (Fig. 2), and it is slightly blue-shifted as compared to the S_0–S_1 transition (Table S1, ESI†).

Consistent with the above, the same is found in the emission spectra, which show a broad phosphorescence emission at 780 nm for all complexes, with similar lifetimes of *ca.* 500 ns and low photoluminescence quantum yields (PLQY, >1%, Fig. 2). Under aerated conditions, a second emission band at higher energy is additionally distinguishable for complexes **2** and **4**, albeit with very low intensity (Fig. 2). Reminiscent of what we observed in our previous study,[45] we attribute this behaviour to a dual emission process. Further experimental evidence of both fluorescence and phosphorescence emissions has been obtained by recording the luminescence response of the complexes under air atmosphere, which shows only a decrease in the NIR signal due to the quenching of the emitting triplet state by molecular oxygen (Fig. S3–S5, ESI†). The corresponding nanosecond lifetime of this luminescence signal confirms the fluorescence nature of this emission, which has also been reported for platinum complexes exhibiting a weak electronic interaction between the d orbitals of the metal and the π-orbitals of the organic ligand.[49–52] Furthermore, theory predicts phosphorescence in the NIR spectral region whereas fluorescence should appear at much shorter wavelengths (Table S1, ESI†), confirming the experimental assignment. In Fig. 2 and Table S2 (ESI†), we report computed data for the ISC process. The two most interesting molecules are likely **2** and **3**. In both, one notices large S_1–T_1 gaps of −0.77 eV associated with SOC of *ca.* 16 cm^{-1}, that is, large gaps and moderate SOC for Pt-bearing systems. In **2**, the S_1–T_2 gap is +0.12 eV, but this small uphill process is likely available, especially since the associated SOC is 94 cm^{-1}, *i.e.*, it is likely that some ISC takes place towards the second triplet state due to thermal effects. In **3**, this state is almost perfectly aligned with S_1 (−0.02 eV gap) and associated with a large SOC of 74 cm^{-1} as well, indicating a very efficient ISC, consistent with the absence of fluorescence in the experiment.

In contrast, modifying the position of the electron donor group on the naphthyl unit, as in complexes **5** and **6**, induces a noticeable change for both the absorption and emission properties. Indeed, while the absorption spectra of these complexes show a similar intensity as their isoquinoline substituted analogues, they undergo a redshift of *ca.* 50 nm for the lowest energy band with a noticeable difference between the methoxy and dimethyl amino substituents, indicating a stronger impact of these functional groups on the excited-state properties (Fig. 2). The donating groups of **5** and **6** indeed play an active role in the EDD plots (Fig. 2 and Fig. S34, S35, ESI†) contrasting with dyes **2** and **3**. Under aerated conditions, the emission spectra of complexes **5** and **6** shows a phosphorescence band at *ca.* 770 nm with the same profile as that for complexes **2** and **3**, with also a higher energy emission band centred at 575 and 620 nm for **5** and **6**, respectively, much higher in intensity than the ones hardly observed in the case of complexes **2** and **3**. Interestingly, increasing the electric dipole moment of the substituent in complex **6** with the dimethyl amino group impacts significantly the intensity of the dual emission process since the fluorescence/phosphorescence ratio becomes higher than for complex **5**; the fluorescence of **6** remaining distinguishable even when the measurement is performed under degassed conditions, which is not the case for complex **5** (Fig. S3–S5, ESI†). This suggests that the radiative deexcitation of the singlet excited-state, in competition with ISC, is favoured when it acquired higher ILCT character. This aspect can be also evidenced by the lifetimes of the fluorescence emission which is longer for complex **6** in comparison with complex **5**, respectively (Fig. 2). Additional insights into these experimental outcomes are provided by theory (Table S1, ESI†), which first predicts the fluorescence (phosphorescence) at 523 and 544 (780) nm for **5** and **6**, respectively, confirming the experimental assignments, although the theoretical emission of **6** is too blue shifted. Second, for **5** the S_1–T_1 and S_1–T_2 gaps (on the optimal S_1 geometry) are, respectively, −0.73 eV and +0.31 eV. Even given the error of theory, it therefore suggests that ISC to the second triplet state is difficulty achievable, and only the S_1–T_1 channel is open. For that transition, we compute a rather small SOC matrix element of 10.7 cm^{-1}. In **6**, the gaps are similar, −0.70 and +0.34 eV, but the SOC is significantly smaller at 7.8 cm^{-1}. These values are qualitatively consistent with the clear observation of fluorescence in **5–6**, and its absence in **3**, which present notably different ISC features (*vide supra*).

Increasing the electron donor nature of the anciallary ligand in complexes **5-acac** and **6-acac**, by replacing the triphenyl phosphine and chloride ones with an acac unit, redshifts their absorption spectra which suggest a slight increase of the role of the metal in the lowest energy band. A small change can indeed be seen in Fig. 2, although the global topology of the transition is preserved. The acac ligand also impacts the phosphorescence emission with a hypsochromic shift when compared to their PPh_3/Cl analogue complexes ($\Delta\lambda_{em}$ = 39 and 19 nm for **5-acac** and **6-acac**, respectively, Fig. 2). This is also associated with a longer lifetime of the emission, also in line with more pronounced MLCT character of the triplet excited-state.

Ground- and excited-state chiroptical properties

The impact of the substituent position and the type of ancillary ligands on the chiroptical properties was also investigated both in the ground and excited states of the complexes using ECD and CPL characterization techniques. As depicted in Fig. 3, the ECD spectra of all compounds display obvious similar responses at the high energy region with a bisignate signal at *ca.* 270 nm, which is reminiscent of the binaphthyl ECD-type signature.[53] This characteristic signal is also found in previously reported ECD spectra of related platinum complexes,[22] as well as in the simulated ECD spectra of complexes **1**, **3**, **5** and **6** (Fig. S36–S39, ESI†) and allow the absolute configuration of these new derivatives to be assigned: the ECD spectrum with the positive → negative couplet corresponds to the *M*-enantiomers while the mirror-image signal is for the *P*-enantiomers.

Open Access Article. Published on 06 September 2024. Downloaded on 1/22/2026 4:13:36 PM.
This article is licensed under a Creative Commons Attribution-NonCommercial 3.0 Unported Licence.

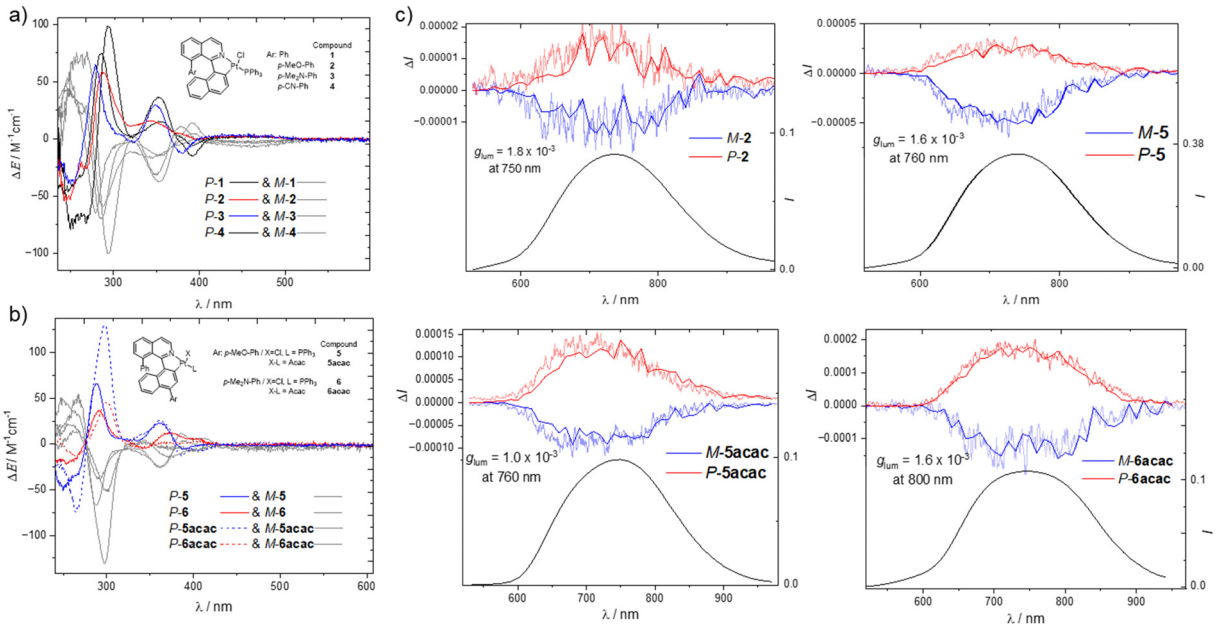

Fig. 3 (a) ECD of complexes **1**, **2**, **3** and **4**, and (b) of complexes **5**, **6**, **5acac** and **6acac** (right) recorded in dichloromethane at 298 K ([c] $\sim 10^{-5}$ M); (c) CPL of complexes **2** and **5** (top), and **5acac** and **6acac** (bottom) recorded in toluene solution at 298 K ([c] $\sim 10^{-5}$ M. For CPL measurements, the faded spectra are the ones directly measured, and the spectra in solid lines are corrected using a calibration curve for the detector.

In addition to this couplet, complexes **1–3** display very similar ECD responses with a set of three signals at 355, 392 and a broader one between 400 and 500 nm, respectively, positive, negative and positive. The corresponding intensity of these bands decreases when going to lower energy, ranging from up 25 to 2 M^{-1} cm^{-1}, resulting in similar absorption dissymmetry factors, g_{abs}, of *ca.* 6.0×10^{-4} at 460 nm.

Changing the position of the donor group on the naphthalene unit in complexes **5** and **6** does not significantly affect the couplet signal at 270 nm, but clearly impacts the intensity of the lower energy bands in a similar way for both methoxy and dimethyl amino groups, which evidences the role of the donor group in these optical transitions. For instance, the positive signal at 340 nm for compound **2** almost disappears in the case of compound **5** concomitantly to an intensity increase of the signal at 370 nm and an almost complete vanishing of the lowest energy broad band, as illustrated by the obtained zero value of g_{abs} at 460 nm. Finally, the replacement of the triphenlphosphine and chloro ligands by the acac one in complexes **5-acac** and **6-acac** does not tune the overall shape of the obtained ECD spectra but rather impacts the intensity of the involved bands, in a similar manner for both compounds. As an illustration, **5-acac** shows a strong increase in the band at 300 nm (from *ca.* 60 to 110 M^{-1} cm^{-1} when comparing complexes **5** and **5-acac**, respectively), together with a less pronounced but clearly distinguishable increase of the low energy signal, resulting in g_{abs} of *ca.* 5.0×10^{-4} at 460 nm.

In line with the NIR luminescence obtained for these new Pt complexes, all of these complexes display CP phosphorescence with mirror-image responses that extent lower than 900 nm, as depicted in Fig. 3 for complexes **2**, **5**, **5-acac**, and **6-acac**. The chiral platinum complexes exhibited almost constant g_{Lum} values between 650 and 900 nm with values of *ca.* 1.0-2.0 $\times 10^{-3}$ (Fig. S32, ESI†), showing a limited influence of both the electron donor group and the ancillary ligands on the intensity of the CPL. Among the complexes, only **6** shows a different behavior than the other systems, with a weak dual CPL at 570 and 760 nm, opposite in sign (Fig. S33, ESI†), presumably linked to the significant dual emission observed for this compound.

Accordingly, a first CP fluorescence can be observed, arising mainly from ILCT transitions, followed by a lowest energy CP phosphorescence involving MLCT, and presumably explaining the sign inversion observed between these two responses. The introduction of the acac ligands in **5-acac** and **6-acac** does not significantly modulate the CPL intensity, and the overall CPL brightness (B_{CPL}) of these complexes falls in the range of 10^{-2} M^{-1} cm^{-1}.[13,14] These values are rather weak in the context of molecular CPL emitters,[2,13,54] which is mainly attributed to the low PLQY of the complexes. However, these results represent an interesting example of NIR CPL, among the most redshifted reported to date for chiral luminophores based on organic and platinum complexes.

Conclusions

In conclusion, we extended the family of NIR CPL molecular emitters by designing innovative chiral platinum complexes displaying phosphorescence around 750–800 nm. Through molecular engineering around a common platinum arylisoquinolines core, we show that the presence of donor groups on both the organic ligand and the metallic ion strongly impacts the interplay between the ILCT and the MLCT transitions,

Open Access Article. Published on 06 September 2024. Downloaded on 1/22/2026 4:13:36 PM. This article is licensed under a Creative Commons Attribution-NonCommercial 3.0 Unported Licence.

promoting a significant dual emission process involving a fluorescence signal between 500 and 700 nm. The later process appears firmly linked to the position of the electron donor substituents on the structure and is favoured when methoxy and amino-donor groups are on the naphthyl unit in complexes **5** and **6**. Such behavior was linked to singlet–triplet excited-state energy gaps and SOC elements, hence to the ISC, for which methoxy and amino donor groups tend to maintain large S_1–T_1 gaps (>-0.77 eV) associated with rather small SOC (<10 cm^{-1}). In comparison, when these donor groups are on the isoquinoline moiety or when an acac ligand is introduced on the metallic ion, the ISC efficiency increases, ultimately favouring phosphorescence emission. While these combined experimental and theoretical investigations reveal the crucial role played by the extended π-helical donor acceptor ligand on the unpolarized emission of these new complexes, these factors seem less crucial for the chiroptical properties. Indeed, this family of chiral molecular emitters afforded NIR CPL at wavelength lower than 900 nm, with dissymmetry factor up to *ca.* 2.0×10^{-3}, which is a significant value for this low energy region. We hope that this investigation may offer new opportunities to design innovative and efficient NIR CPL emitters.

Data availability

The data supporting this article have been included as part of the ESI.†

Conflicts of interest

There are no conflicts to declare.

Acknowledgements

We acknowledge the Ministère de l'Education Nationale, de la Recherche et de la Technologie, the Centre National de la Recherche Scientifique (CNRS). This project is cofunded by the European Union (ERC), SHIFUMI, 101041516 (L. F.). A. R. is grateful to the Consejo Superior de Investigaciones Científicas (CSIC, grant 202080I005) and the Spanish Ministerio de Ciencia e Innovación for financial support (PID2019-106358GB-C21 and doctoral fellowship PRE2020-092646 for P. V.-D.). Views and opinions expressed are however those of the author(s) only and do not necessarily reflect those of the European Union or the European Research Council. Neither the European Union nor the granting authority can be held responsible for them. The Caphter facility (ScanMAT, UMS 2001, Université de Rennes 1 – Campus de Beaulieu) is acknowledged for the photoluminescence characterizations of the compounds. This research used resources of the GLiCID Computing Facility (Ligerien Group for Intensive Distributed Computing, https://doi.org/10.60487/glicid, Pays de la Loire, France).

Notes and references

1 R. Carr, N. H. Evans and D. Parker, Lanthanide complexes as chiral probes exploiting circularly polarized luminescence, *Chem. Soc. Rev.*, 2012, **41**, 7673–7686.
2 J. M. Han, S. Guo, H. Lu, S. J. Liu, Q. Zhao and W. Huang, Recent Progress on Circularly Polarized Luminescent Materials for Organic Optoelectronic Devices, *Adv. Opt. Mater.*, 2018, **6**, 1800538.
3 B. Kunnen, C. Macdonald, A. Doronin, S. Jacques, M. Eccles and I. Meglinski, Application of circularly polarized light for non-invasive diagnosis of cancerous tissues and turbid tissue-like scattering media, *J. Biophotnics*, 2015, **8**, 317–323.
4 M. Lindemann, G. Xu, T. Pusch, R. Michalzik, M. R. Hofmann, I. Žutić and N. C. Gerhardt, Ultrafast spin-lasers, *Nature*, 2019, **568**, 212–215.
5 L. E. MacKenzie and R. Pal, Circularly polarized lanthanide luminescence for advanced security inks, *Nat. Rev. Chem.*, 2021, **5**, 109–124.
6 T. Novikova, A. Pierangelo, S. Manhas, A. Benali, P. Validire, B. Gayet and A. D. Martino, The origins of polarimetric image contrast between healthy and cancerous human colon tissue, *Appl. Phys. Lett.*, 2013, **102**, 241103.
7 H. Wang, L. Liu and C. Lu, CPLC: Visible Light Communication based on Circularly Polarized Light, *Proc. Comput. Sci.*, 2018, **131**, 511–519.
8 B. Doistau, J. R. Jimenez and C. Piguet, Beyond Chiral Organic (p-Block) Chromophores for Circularly Polarized Luminescence: The Success of d-Block and f-Block Chiral Complexes, *Front. Chem.*, 2020, **8**, 555.
9 L. E. MacKenzie and R. Pal, Circularly polarized lanthanide luminescence for advanced security inks, *Nat. Rev. Chem.*, 2020, **5**, 109–124.
10 O. G. Willis, A. Pucci, E. Cavalli, F. Zinna and L. Di Bari, Intense 1400–1600 nm circularly polarised luminescence from homo- and heteroleptic chiral erbium complexes, *J. Mater. Chem. C*, 2023, **11**, 5290–5296.
11 O. G. Willis, F. Zinna and L. Di Bari, NIR-Circularly Polarized Luminescence from Chiral Complexes of Lanthanides and d-Metals, *Angew. Chem., Int. Ed.*, 2023, **62**, e202302358.
12 F. Zinna and L. Di Bari, Lanthanide Circularly Polarized Luminescence: Bases and Applications, *Chirality*, 2015, **27**, 1–13.
13 L. Arrico, L. Di Bari and F. Zinna, Quantifying the Overall Efficiency of Circularly Polarized Emitters, *Chem. – Eur. J.*, 2021, **27**, 2920–2934.
14 Y. Nagata and T. Mori, Irreverent Nature of Dissymmetry Factor and Quantum Yield in Circularly Polarized Luminescence of Small Organic Molecules, *Front. Chem.*, 2020, **8**, 448.
15 J. R. Brandt, F. Salerno and M. J. Fuchter, The added value of small-molecule chirality in technological applications, *Nat. Rev. Chem.*, 2017, **1**, 0045.
16 J. R. Brandt, X. Wang, Y. Yang, A. J. Campbell and M. J. Fuchter, Circularly Polarized Phosphorescent Electroluminescence with a High Dissymmetry Factor from

Open Access Article. Published on 06 September 2024. Downloaded on 1/22/2026 4:13:36 PM.
This article is licensed under a Creative Commons Attribution-NonCommercial 3.0 Unported Licence.

PHOLEDs Based on a Platinahelicene, *J. Am. Chem. Soc.*, 2016, **138**, 9743–9746.

17 S. Feuillastre, M. Pauton, L. Gao, A. Desmarchelier, A. J. Riives, D. Prim, D. Tondelier, B. Geffroy, G. Muller, G. Clavier and G. Pieters, Design and Synthesis of New Circularly Polarized Thermally Activated Delayed Fluorescence Emitters, *J. Am. Chem. Soc.*, 2016, **138**, 3990–3993.

18 J. Gilot, R. Abbel, G. Lakhwani, E. W. Meijer, A. P. H. J. Schenning and S. C. J. Meskers, Polymer Photovoltaic Cells Sensitive to the Circular Polarization of Light, *Adv. Mater.*, 2010, **22**, E131–E134.

19 P. Josse, L. Favereau, C. Shen, S. Dabos-Seignon, P. Blanchard, C. Cabanetos and J. Crassous, Enantiopure versus Racemic Naphthalimide End-Capped Helicenic Non-fullerene Electron Acceptors: Impact on Organic Photovoltaics Performance, *Chem. – Eur. J.*, 2017, **23**, 6277–6281.

20 M. Schulz, M. Mack, O. Kolloge, A. Lutzen and M. Schiek, Organic photodiodes from homochiral l-proline derived squaraine compounds with strong circular dichroism, *Phys. Chem. Chem. Phys.*, 2017, **19**, 6996–7008.

21 Y. Yang, R. C. da Costa, M. J. Fuchter and A. J. Campbell, Circularly polarized light detection by a chiral organic semiconductor transistor, *Nat. Photon*, 2013, **7**, 634–638.

22 Y. Yang, R. C. da Costa, D.-M. Smilgies, A. J. Campbell and M. J. Fuchter, Induction of Circularly Polarized Electroluminescence from an Achiral Light-Emitting Polymer via a Chiral Small-Molecule Dopant, *Adv. Mater.*, 2013, **25**, 2624–2628.

23 X. Li, Y. Xie and Z. Li, The Progress of Circularly Polarized Luminescence in Chiral Purely Organic Materials, *Adv. Photonics Res.*, 2021, **2**, 2000136.

24 N. Liang, C. Cao, Z. Xie, J. Liu, Y. Feng and C.-J. Yao, Advances in near-infrared circularly polarized luminescence with organometallic and small organic molecules, *Mater. Today*, 2024, **75**, 309–333.

25 J. Bosson, G. M. Labrador, C. Besnard, D. Jacquemin and J. Lacour, Chiral Near-Infrared Fluorophores by Self-Promoted Oxidative Coupling of Cationic Helicenes with Amines/Enamines, *Angew. Chem., Int. Ed.*, 2021, **60**, 8733–8738.

26 J. Bosson, G. M. Labrador, S. Pascal, F. A. Miannay, O. Yushchenko, H. Li, L. Bouffier, N. Sojic, R. C. Tovar, G. Muller, D. Jacquemin, A. D. Laurent, B. Le Guennic, E. Vauthey and J. Lacour, Physicochemical and Electronic Properties of Cationic [6]Helicenes: from Chemical and Electrochemical Stabilities to Far-Red (Polarized) Luminescence, *Chem. – Eur. J.*, 2016, **22**, 18394–18403.

27 I. H. Delgado, S. Pascal, A. Wallabregue, R. Duwald, C. Besnard, L. Guenee, C. Nancoz, E. Vauthey, R. C. Tovar, J. L. Lunkley, G. Muller and J. Lacour, Functionalized cationic [4]helicenes with unique tuning of absorption, fluorescence and chiroptical properties up to the far-red range, *Chem. Sci.*, 2016, **7**, 4685–4693.

28 K. Dhbaibi, L. Favereau, M. Srebro-Hooper, M. Jean, N. Vanthuyne, F. Zinna, B. Jamoussi, L. Di Bari, J. Autschbach and J. Crassous, Exciton coupling in diketopyrrolopyrrole–helicene derivatives leads to red and near-infrared circularly polarized luminescence, *Chem. Sci.*, 2018, **9**, 735–742.

29 K. Dhbaibi, C. Shen, M. Jean, N. Vanthuyne, T. Roisnel, M. Górecki, B. Jamoussi, L. Favereau and J. Crassous, Chiral Diketopyrrolopyrrole-Helicene Polymer With Efficient Red Circularly Polarized Luminescence, *Front. Chem.*, 2020, **8**, 237.

30 R. Duwald, J. Bosson, S. Pascal, S. Grass, F. Zinna, C. Besnard, L. Di Bari, D. Jacquemin and J. Lacour, Merging polyacenes and cationic helicenes: from weak to intense chiroptical properties in the far red region, *Chem. Sci.*, 2020, **11**, 1165–1169.

31 R. Duwald, S. Pascal, J. Bosson, S. Grass, C. Besnard, T. Bürgi and J. Lacour, Enantiospecific Elongation of Cationic Helicenes by Electrophilic Functionalization at Terminal Ends, *Chem. – Eur. J.*, 2017, **23**, 13596–13601.

32 J. Feng, L. Fu, H. Geng, W. Jiang and Z. Wang, Designing a near-infrared circularly polarized luminescent dye by dissymmetric spiro-fusion, *Chem. Commun.*, 2020, **56**, 912–915.

33 J. Jimenez, C. Diaz-Norambuena, S. Serrano, S. C. Ma, F. Moreno, B. L. Maroto, J. Banuelos, G. Muller and S. de la Moya, BINOLated aminostyryl BODIPYs: a workable organic molecular platform for NIR circularly polarized luminescence, *Chem. Commun.*, 2021, **57**, 5750–5753.

34 R. Tarrieu, I. H. Delgado, F. Zinna, V. Dorcet, S. Colombel-Rouen, C. Crevisy, O. Basle, J. Bosson and J. Lacour, Hybrids of cationic [4]helicene and N-heterocyclic carbene as ligands for complexes exhibiting (chir)optical properties in the far red spectral window, *Chem. Commun.*, 2021, **57**, 3793–3796.

35 T. Biet, T. Cauchy, Q. Sun, J. Ding, A. Hauser, P. Oulevey, T. Bürgi, D. Jacquemin, N. Vanthuyne, J. Crassous and N. Avarvari, Triplet state CPL active helicene–dithiolene platinum bipyridine complexes, *Chem. Commun.*, 2017, **53**, 9210–9213.

36 G. Fu, Y. He, W. Li, B. Wang, X. Lü, H. He and W.-Y. Wong, Efficient polymer light-emitting diodes (PLEDs) based on chiral [Pt(C^N)(N^O)] complexes with near-infrared (NIR) luminescence and circularly polarized (CP) light, *J. Mater. Chem. C*, 2019, **7**, 13743–13747.

37 E. Anger, M. Rudolph, L. Norel, S. Zrig, C. Shen, N. Vanthuyne, L. Toupet, J. A. G. Williams, C. Roussel, J. Autschbach, J. Crassous and R. Réau, Multifunctional and Reactive Enantiopure Organometallic Helicenes: Tuning Chiroptical Properties by Structural Variations of Mono- and Bis(platinahelicene)s, *Chem. – Eur. J.*, 2011, **17**, 14178–14198.

38 L. Norel, M. Rudolph, N. Vanthuyne, J. A. G. Williams, C. Lescop, C. Roussel, J. Autschbach, J. Crassous and R. Réau, Metallahelicenes: Easily Accessible Helicene Derivatives with Large and Tunable Chiroptical Properties, *Angew. Chem., Int. Ed.*, 2010, **49**, 99–102.

39 N. Saleh, C. Shen and J. Crassous, Helicene-based transition metal complexes: synthesis, properties and applications, *Chem. Sci.*, 2014, **5**, 3680–3694.

40 C. Shen, E. Anger, M. Srebro, N. Vanthuyne, K. K. Deol, T. D. Jefferson, G. Muller, J. A. G. Williams, L. Toupet,

Open Access Article. Published on 06 September 2024. Downloaded on 1/22/2026 4:13:36 PM.
This article is licensed under a Creative Commons Attribution-NonCommercial 3.0 Unported Licence.

C. Roussel, J. Autschbach, R. Reau and J. Crassous, Straightforward access to mono- and bis-cycloplatinated helicenes displaying circularly polarized phosphorescence by using crystallization resolution methods, *Chem. Sci.*, 2014, **5**, 1915–1927.

41 A. Zampetti, A. Minotto and F. Cacialli, Near-Infrared (NIR) Organic Light-Emitting Diodes (OLEDs): Challenges and Opportunities, *Adv. Funct. Mater.*, 2019, **29**, 1807623.

42 K. Zhang, T. Y. Wang, T. W. Wu, Z. M. Ding, Q. Zhang, W. G. Zhu and Y. Liu, An effective strategy to obtain near-infrared emission from shoulder to shoulder-type binuclear platinum(ii) complexes based on fused pyrene core bridged isoquinoline ligands, *J. Mater. Chem. C*, 2021, **9**, 2282–2290.

43 Y. Zhang, Y. Wang, J. Song, J. Qu, B. Li, W. Zhu and W.-Y. Wong, Near-Infrared Emitting Materials via Harvesting Triplet Excitons: Molecular Design, Properties, and Application in Organic Light Emitting Diodes, *Adv. Opt. Mater.*, 2018, **6**, 1800466.

44 K. Tuong Ly, R.-W. Chen-Cheng, H.-W. Lin, Y.-J. Shiau, S.-H. Liu, P.-T. Chou, C.-S. Tsao, Y.-C. Huang and Y. Chi, Near-infrared organic light-emitting diodes with very high external quantum efficiency and radiance, *Nat. Photon*, 2017, **11**, 63–69.

45 P. Vázquez-Domínguez, O. Journaud, N. Vanthuyne, D. Jacquemin, L. Favereau, J. Crassous and A. Ros, Helical donor–acceptor platinum complexes displaying dual luminescence and near-infrared circularly polarized luminescence, *Dalton Trans.*, 2021, **50**, 13220–13226.

46 The helicene racemates were resolved into the enantiopure forms by semipreparative CSP-HPLC separation (see Supp. Inf.).

47 Z. Domínguez, R. López-Rodríguez, E. Álvarez, S. Abbate, G. Longhi, U. Pischel and A. Ros, Azabora[5]helicene Charge-Transfer Dyes Show Efficient and Spectrally Variable Circularly Polarized Luminescence, *Chem. – Eur. J.*, 2018, **24**, 12660–12668.

48 V. V. Sivchik, A. I. Solomatina, Y.-T. Chen, A. J. Karttunen, S. P. Tunik, P.-T. Chou and I. O. Koshevoy, Halogen Bonding to Amplify Luminescence: A Case Study Using a Platinum Cyclometalated Complex, *Angew. Chem., Int. Ed.*, 2015, **54**, 14057–14060.

49 Y. Y. Chia and M. G. Tay, An insight into fluorescent transition metal complexes, *Dalton Trans.*, 2014, **43**, 13159–13168.

50 F. Geist, A. Jackel and R. F. Winter, Dual ligand-based fluorescence and phosphorescence emission at room temperature from platinum thioxanthonyl complexes, *Dalton Trans.*, 2015, **44**, 3974–3987.

51 F. Geist, A. Jackel and R. F. Winter, Ligand Based Dual Fluorescence and Phosphorescence Emission from BODIPY Platinum Complexes and Its Application to Ratiometric Singlet Oxygen Detection, *Inorg. Chem.*, 2015, **54**, 10946–10957.

52 Y. Liu, H. Guo and J. Zhao, Ratiometric luminescent molecular oxygen sensors based on uni-luminophores of C^N Pt(ii)(acac) complexes that show intense visible-light absorption and balanced fluorescence/phosphorescence dual emission, *Chem. Commun.*, 2011, **47**, 11471–11473.

53 L. Di Bari, G. Pescitelli and P. Salvadori, Conformational Study of 2,2′-Homosubstituted 1,1′-Binaphthyls by Means of UV and CD Spectroscopy, *J. Am. Chem. Soc.*, 1999, **121**, 7998–8004.

54 H. Tanaka, Y. Inoue and T. Mori, Circularly Polarized Luminescence and Circular Dichroisms in Small Organic Molecules: Correlation between Excitation and Emission Dissymmetry Factors, *ChemPhotoChem*, 2018, **2**, 386–402.